

Raman- and infrared-active phonons in YBaCuFeO_5 : Experiment and lattice dynamics

Y. K. Atanassova, V. N. Popov, G. G. Bogachev, and M. N. Iliev
Faculty of Physics, Sofia University, 1126 Sofia, Bulgaria

C. Mitros, V. Psycharis, and M. Pissas

Institute of Materials Science, National Center for Scientific Research "Democritos," 15310 Attiki, Greece
 (Received 27 July 1992; revised manuscript received 29 December 1992)

The results of polarized Raman scattering, far-infrared (FIR) absorption, Kramers-Kronig analysis of FIR reflectance, and lattice-dynamical calculations of the perovskitelike compound YBaCuFeO_5 (space group $P4mm$) are reported. All 16 Raman- and infrared-active Γ -point phonons ($6A_1 + 2B_1 + 8E$) have been identified and assigned to definite atomic vibrations in close comparison with the structurally similar tetragonal $\text{YBa}_2\text{Cu}_3\text{O}_6$ system. The appearance of an additional strong Raman line at 576 cm^{-1} is discussed in terms of disorder-induced Raman scattering. The normal-mode frequencies are in reasonable agreement with the results of lattice-dynamical calculations in the framework of a shell model with parameters extracted from several metallic oxides and perovskite compounds.

INTRODUCTION

The perovskitelike antiferromagnetic compound with layer structure $\text{YBaCuFeO}_{5+\delta}$ was isolated by Er-Rakho *et al.*¹ and characterized by Rietveld refinements of the neutron diffraction pattern using the $P4mm$ space group with Cu and Fe atoms, distributed at the $1(b1)$ and $1(b2)$ sites. Later, Meyer *et al.*² on the basis of Mössbauer spectra analysis concluded that the $1(b1)$ site is occupied only with iron and the $1(b2)$ site with copper. Recently, Mitros *et al.*³ have fitted the x-ray diffraction data using Rietveld profile technique in the centrosymmetric space group $P4/mmm$ and the obtained interatomic distances were very close to that given in Ref. 1. In both cases ($P4mm$ or $P4/mmm$ space group) the structure of YBaCuFeO_5 [Fig. 1(a)] is very similar to the one of tetragonal $\text{YBa}_2\text{Cu}_3\text{O}_6$ (the so-called 123 system) [Fig. 1(b)]. Indeed, the former structure(s) could be obtained by the latter ($P4/mmm$) by removing the Cu1 layers and replacing one half of the Cu2 atoms by Fe.

Among the few reports¹⁻⁴ on the properties of YBaCuFeO_5 there are, to our knowledge, no published results on the phonon spectra. Such studies, in particular the investigation of the Raman and infrared (IR) spectra, could help to determine the space group as far as different numbers of Raman- and/or IR-allowed phonons are expected with the $P4mm$ and $P4/mmm$ structures. The comparison with the phonon modes of $\text{YBa}_2\text{Cu}_3\text{O}_{6+\delta}$ is also of significant interest because of the existence of similarities in the structures of YBaCuFeO_5 and $\text{YBa}_2\text{Cu}_3\text{O}_{6+\delta}$.

In this work we report polarized Raman spectra of YBaCuFeO_5 , obtained in exact scattering configurations from single microcrystals, as well as nonpolarized far-infrared (FIR) transmission and reflectance spectra of the same material. It is shown that the Raman and infrared phonon lines correspond to the normal modes expected for the $P4mm$ and not for the $P4/mmm$ structure. In

close comparison with the well-known spectra of $\text{YBa}_2\text{Cu}_3\text{O}_6$ some of the lines are assigned to definite atomic vibrations. These assignments are further confirmed by the results of lattice dynamical calculations⁵ carried out using a shell model within the $P4mm$ structure. The rather good agreement between the calculated and experimentally obtained phonon frequencies allows the identification all Γ -point phonons ($6A_1 + 2B_1 + 8E$) of the $P4mm$ structure of YBaCuFeO_5 .

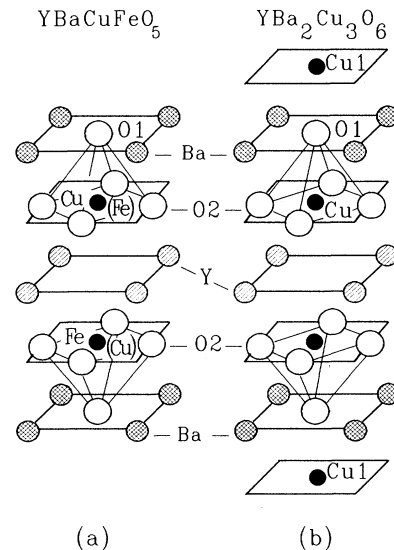


FIG. 1. Elementary cell of (a) YBaCuFeO_5 ($P4/mmm$ or $P4mm$) and (b) $\text{YBa}_2\text{Cu}_3\text{O}_6$ ($P4/mmm$). In the case of the $P4/mmm$ structure of YBaCuFeO_5 the Fe and Cu atoms are randomly distributed at the two equivalent $2(h)$ sites and in the case of $P4mm$ Fe atoms occupy $1(b1)$ and Cu- $1(b2)$ sites.

SAMPLES AND EXPERIMENT

The YBaCuFeO_5 material was prepared from stoichiometric mixture of Y_2O_3 , BaCO_3 , CuO , and Fe_2O_3 , first at 960°C . The powders were pressed into pellets and sintered for 110 h at 980°C in air with intermediate regrindings. The x-ray powder diffraction data were collected in the range 20° – 120° using a Siemens D500 diffractometer with $\text{Cu } K\alpha$ radiation and diffracted beam monochromator. The x-ray diffraction patterns of the sample used in Raman and infrared experiments was refined using the Rietveld technique in space group $P4/mmm$ ($a=3.87382 \text{ \AA}$, $c=7.6623 \text{ \AA}$),³ the Fe and Cu atoms randomly occupying the two $2(h)$ sites or in $P4mm$ space group [$a=3.867(7) \text{ \AA}$, $c=7.661(5) \text{ \AA}$]⁴ using site $1(b1)$ for iron and site $1(b2)$ for copper. The interatomic distances^{1,3} in YBaCuFeO_5 are given in Table I together with the corresponding distances⁶ in $\text{YBa}_2\text{Cu}_3\text{O}_{6+\delta}$.

The visual observation through an optical microscope of the polished surface of a pellet (in polarized light) showed differently oriented mostly elongated microcrystals of 5 to 20 μm and 10 to 50 μm in the shortest and in the longest dimensions, respectively. It has been established by TEM analysis of grains constituting the pellet that similarly to $\text{YBa}_2\text{Cu}_3\text{O}_{6+\delta}$ the microcrystals of YBaCuFeO_5 grew in the form of platelets parallel to the ab planes, and hence the long sides of their elongated projections are along a direction x in the ab planes. The direction that is perpendicular to x (further denoted as z) lies in a plane that includes also the c axis. As long as the ab plane is the plane of easy cleavage, it is exhibited by most of the grains on the surface of a freshly broken pellet.

The polarized Raman spectra were measured in the backward scattering configuration by means of a triple spectrometer (Microdil 28) in conjunction with an optical microscope (objective $\times 100$) and an optical multichannel analyzer. An improved software was used for processing the very weak signals. In order to avoid overheating, the laser power ($\lambda_L=514.5 \text{ nm}$) at the focus spot (1–2 μm diameter) was kept below 0.2 mW. The typical acquisition times were 5000 s. The spectra collected from different microcrystals were almost identical.

TABLE I. Comparison of the interatomic distances in YBaCuFeO_5 , obtained by neutron (Ref. 1) and x-ray (Ref. 3) diffraction, and in tetragonal $\text{YBa}_2\text{Cu}_3\text{O}_{6+\delta}$ (Ref. 6).

Bond	YBaCuFeO_5		$\text{YBa}_2\text{Cu}_3\text{O}_{6+\delta}$
	$P4mm$ (Ref. 1)	$P4/mmm$ (Ref. 3)	$P4/mmm$ (Ref. 6)
Y-O2	2.383	2.39	2.40
Cu-O2	1.966	1.96	1.95
Fe-O2	1.999	1.98	
Cu-O1	2.130	2.12	2.43
Fe-O1	1.998	1.99	
Cu1-O1			1.80
Cu-Cu		3.41	3.27
Cu-Fe	3.559	3.55	
Ba-O1	2.753	2.74	2.77

The infrared transmittance spectra were measured between 140 and 700 cm^{-1} by means of a Fourier spectrometer (Bomem DA3) using pellets of CsI containing 1/200 part of finely grinded YBaCuFeO_5 pressed for 5 min at 15 kbar at room temperature. The reflectance spectra were measured from the polished surface of polycrystalline YBaCuFeO_5 between 50 and 4500 cm^{-1} .

LATTICE DYNAMICAL CALCULATIONS

Lattice dynamical calculations⁵ were carried out using a shell model in order to remove the uncertainties in the assignment of some of the observed frequencies. In this model the ionic interactions consist of long-range Coulomb parts and short-range ones in the form of Born-Mayer potentials. In order to account for the electronic polarizability of the ions, each ion is represented by a charged core and a charged rigid spherical shell, enabled to move relative to the core and coupled to it via a spring. In the present model the ionic charges were fixed at their nominal values. The Born-Mayer parameters for the short-range Cu-O and O-O interactions were transferred from other studied materials: Ca_2CuO_3 and Nd_2CuO_4 ; those for the short-range Ba-O and Y-O interactions were obtained from fits to the dispersion curves of BaO and SrO. The shell charges and the core-shell force constants for the Y, Ba, Cu, and O ions were taken over from the above-mentioned compounds.⁵ These parameters describe fairly well the lattice dynamics of $\text{YBa}_2\text{Cu}_3\text{O}_6$ and served as the basis for our study of the Γ -point phonons of YBaCuFeO_5 . In the latter case, however, the necessary Fe-O interaction parameters were not available and they were determined using the equilibrium conditions; and they were slightly varied in order to provide stability over the entire Brillouin zone.

RESULTS AND DISCUSSION

The comparison between the structures of YBaCuFeO_5 ($P4mm$ of $P4/mmm$) and $\text{YBa}_2\text{Cu}_3\text{O}_6$ ($P4/mmm$) shows that these compounds have some identical structural fragments and have very close interatomic distances.

If the structure of the YBaCuFeO_5 corresponds to the $P4/mmm$ space group, the Y, Cu(Fe), and O2 atoms occupy sites of the same symmetry as in the tetragonal 123 system, whereas the Ba and O1 sites are centers of inversion, and hence the Ba and O1 vibrations are Raman-forbidden (see Table II). Within the space group $P4mm$, all sites of YBaCuFeO_5 become Raman- and simultaneously infrared-active and only the Cu/Fe-O2 out-of-phase B_1 modes are strictly Raman-active and infrared-forbidden (see Table II). In both possible structures of YBaCuFeO_5 , however, the interatomic distances are close to those of $\text{YBa}_2\text{Cu}_3\text{O}_{6+\delta}$, and hence one expects close values of the Raman frequencies and similar polarization dependences for the Raman-active modes related to vibrations of Cu/Fe and O2 atoms.

Figure 2 shows the Raman spectra of YBaCuFeO_5 in $y(zz)\bar{y}$, $y(xx)\bar{y}$, $c(aa)\bar{c}$, $c(bb)\bar{c}$, $c(a+b, a+b)\bar{c}$, and $c(a+b, a-b)\bar{c}$ scattering configurations, where $a+b$ and $a-b$ are two orthogonal directions at an angle of 45°

TABLE II. Site symmetries, Wickoff positions, and irreducible representations for the atoms in YBaCuFeO₅ for space groups *P4mm* and *P4/mmm*.

Atom	Space group	Site symmetry	Wickoff notation	Irreducible representations
Y	<i>P4mm</i>	<i>C</i> _{4v}	1(<i>a</i>)	<i>A</i> ₁ + <i>E</i>
	<i>P4/mmm</i>	<i>D</i> _{4h}	1(<i>b</i>)	<i>A</i> _{2u} + <i>E</i> _u
Ba	<i>P4mm</i>	<i>C</i> _{4v}	1(<i>a</i>)	<i>A</i> ₁ + <i>E</i>
	<i>P4/mmm</i>	<i>D</i> _{4h}	1(<i>a</i>)	<i>A</i> _{2u} + <i>E</i> _u
Fe		<i>C</i> _{4v}	1(<i>b</i> 1)	
Cu	<i>P4mm</i>			2 <i>A</i> ₁ + 2 <i>E</i>
		<i>C</i> _{4v}	1(<i>b</i> 2)	
Cu, Fe	<i>P4/mmm</i>	<i>C</i> _{4v}	2(<i>h</i>)	<i>A</i> _{1g} + <i>E</i> _g + <i>A</i> _{2u} + <i>E</i> _u
O1	<i>P4mm</i>	<i>C</i> _{4v}	1(<i>b</i>)	<i>A</i> ₁ + <i>E</i>
	<i>P4/mmm</i>	<i>D</i> _{4h}	1(<i>c</i>)	<i>A</i> _{2u} + <i>E</i> _u
O2	<i>P4/mmm</i>	<i>C</i> _{2v} ²	2(<i>c</i>)	<i>A</i> ₁ + <i>B</i> ₁ + 2 <i>E</i> + <i>A</i> ₁ + <i>B</i> ₁ + 2 <i>E</i>
	<i>P4/mmm</i>	<i>C</i> _{4v} ^v	2(<i>i</i>)	<i>A</i> _{1g} + <i>B</i> _{1g} + 2 <i>E</i> _g + <i>A</i> _{2u} + <i>B</i> _{2u} + 2 <i>E</i> _u

Mode classification	
	<i>P4mm</i>
Γ_{Raman}	{ 6 <i>A</i> ₁ + 2 <i>B</i> ₁ + 8 <i>E</i> }
Γ_{IR}	
Γ_{acoust}	<i>A</i> ₁ + <i>E</i>
Γ_{acoust}	<i>A</i> ₁ + <i>E</i>
Γ_{silent}	

	<i>P4/mmm</i>
Γ_{Raman}	2 <i>A</i> _{1g} + <i>B</i> _{1g} + 3 <i>E</i> _g
Γ_{IR}	4 <i>A</i> _{2u} + 5 <i>E</i> _u
Γ_{acoust}	<i>A</i> _{2u} + <i>E</i> _u
Γ_{acoust}	<i>A</i> _{2u} + <i>E</i> _u
Γ_{silent}	<i>B</i> _{2u}

	<i>P4mm</i>	<i>P4/mmm</i>
$A_1 \rightarrow \alpha_{xx}^z + \alpha_{yy}^z, \alpha_{zz}^z$	$A_{1g} \rightarrow \alpha_{xx} + \alpha_{yy}, \alpha_{zz}$	
$B_1 \rightarrow \alpha_{xx}^z - \alpha_{yy}^z$	$B_{1g} \rightarrow \alpha_{xx} - \alpha_{yy}$	
$E \rightarrow \alpha_{xz}^x, \alpha_{yz}^y$	$E_u \rightarrow \alpha_{xz}, \alpha_{yz}$	

with respect to a straight edge (assumed to coincide with the *a* or *b* direction) of a plateletlike microcrystal on the as-broken grain surface. Taking into account the definition for the *x*, *y*, and *z* directions, the *y*(*zz*) \bar{y} scattering configuration has to be considered as mainly *b*(*cc*) \bar{b} with a small admixture of [*b*(*ac*) \bar{b} + *b*(*ca*) \bar{b}], the *y*(*xx*) \bar{y} —as mainly [*b*(*aa*) \bar{b} + *a*(*bb*) \bar{a}], and the *y*(*zx*) \bar{y} —as mainly the mixture [*b*(*ca*) \bar{b} + *a*(*cb*) \bar{a}] with a small admixture of [*b*(*aa*) \bar{b} + *a*(*cc*) \bar{a}]. The comparison of the Raman line intensities in the *y*(*zz*) \bar{y} , *y*(*xx*) \bar{y} , and *y*(*zx*) \bar{y} spectra shows that, as a rule, the *A*₁(*A*_{1g}) and *B*₁(*B*_{1g}) lines are much more intensive than the ones of *E*(*E*_g) symmetry. Therefore the small admixture of cross-scattering configurations [where the *E*(*E*_g) lines have to be observed] to the parallel ones, such as *y*(*zz*) \bar{y} or *y*(*xx*) \bar{y} , could be neglected and it is reasonable to assign all lines in the latter spectra to modes of *A*₁(*A*_{1g}) or *B*₁(*B*_{1g}) symmetry.

The most pronounced lines in the Raman spectra with parallel polarizations of the incident and the scattered light are the ones at 180 cm⁻¹ (*xx*-polarized), 214 cm⁻¹ (*zz*), 345 cm⁻¹ (*xx*), 456 cm⁻¹ (*zz*), 576 cm⁻¹ (unpolarized), and at 669 cm⁻¹ (mainly *zz*-polarized). The spectral features in the *y*(*zx*) \bar{y} and *y*(*xz*) \bar{y} spectra, where the *E* modes are expected, are much weaker. The cross-polarized *c*(*a* + *b*, *a* - *b*) \bar{c} spectrum is dominated by the

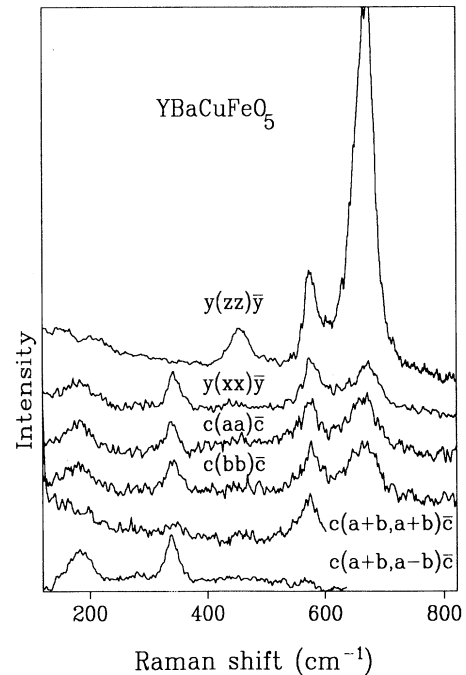


FIG. 2. Polarized Raman spectra of YBaCuFeO₅.

lines at 180 and 345 cm^{-1} . Their strong reduction in the parallel $c(a+b, a+b)\bar{c}$ spectrum is consistent with B_1 (B_{1g} -like) symmetry.

The number of the observed Raman-active modes of YBaCuFeO_5 (six) in parallel polarization is already an indication for a $P4mm$ rather than for a $P4/mmm$ structure where only two Raman-active modes are expected in the zz -polarized spectra.

Two spectra, obtained in $y(zx)\bar{y}$ and $y(xz)\bar{y}$ polarization geometries, are illustrated in Fig. 3. Both spectra are identical and by an order of magnitude weaker than the spectra with parallel incident and scattered polarizations. Weak features are observed at 142, 192, 280, 320, 545, 576, and 669 cm^{-1} . Although only E modes have to be expected in these scattering geometries, some of the lines are certainly due to "polarization leakages" of the much stronger A_1 modes, e.g., the intensive peak at 669 cm^{-1} . The group-theoretical analysis and lattice dynamical calculations⁷ for $\text{YBa}_2\text{Cu}_3\text{O}_6$ yield five E_g modes involving motions of the same atoms which build the elementary cell of YBaCuFeO_5 . Thus the structural similarity and the results of calculations of the lattice dynamics allow us to assign the lines in the cross-polarized Raman spectra to definite modes of E symmetry in YBaCuFeO_5 .

Figure 4 shows the transmission and reflectance spectra of YBaCuFeO_5 . The former has absorption maxima at 192, 238 (weak), 276 (weak), 360, 568, and 650 cm^{-1} and as a whole it is similar to that of the nonmetallic tetragonal $\text{YBa}_2\text{Cu}_3\text{O}_6$ system⁸ where only the A_{2u} and E_u modes are IR allowed. This resemblance indicates that the IR absorption of YBaCuFeO_5 is dominated by the corresponding phonon modes of A_1 and E symmetry. In order to obtain the eigenfrequencies ω_{TO} and ω_{LO} we also carried out a Kramers-Kronig analysis (KKA) of the reflectance data between 50 and 4500 cm^{-1} . The reflectance below 50 cm^{-1} was assumed to be constant and the high-frequency reflection above 4500 cm^{-1} —to be proportional to ω^{-4} , which is an appropriate approximation for insulators. The frequencies of the TO phonons were obtained from the maxima of the $\text{Im}[\epsilon(\omega)]$ curve, while those for the LO phonons—from the maxima of $-\text{Im}[1/\epsilon(\omega)]$, $\epsilon(\omega)$ being the complex dielectric

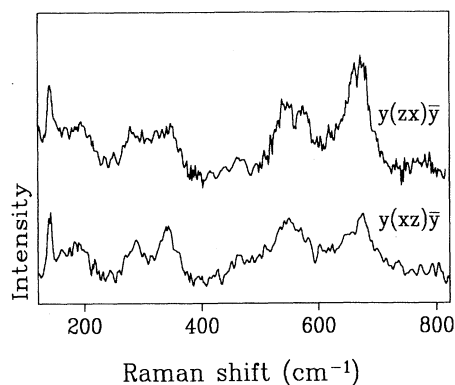


FIG. 3. Polarized Raman spectra of YBaCuFeO_5 in $y(zx)\bar{y}$ and $y(xz)\bar{y}$ polarization configurations.

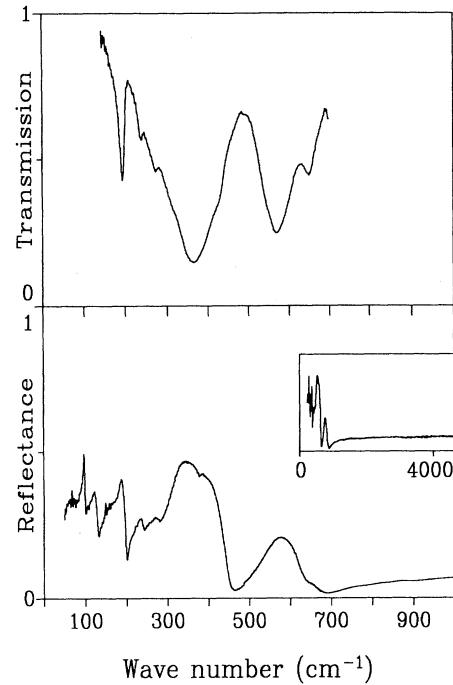


FIG. 4. Transmission and reflectance spectra of YBaCuFeO_5 .

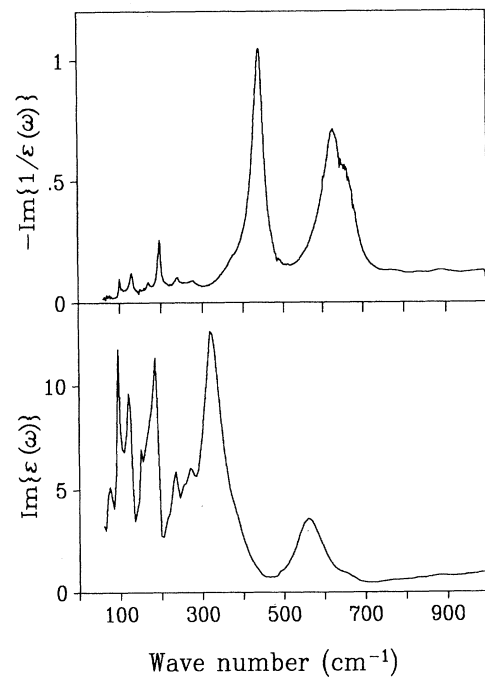


FIG. 5. Curves of $\text{Im}\{\epsilon(\omega)\}$ and $-\text{Im}\{1/\epsilon(\omega)\}$, where $\epsilon(\omega)$ is the complex dielectric function, obtained by Kramers-Kronig analysis. The derived values of TO and LO phonon frequencies are included in Table III.

TABLE III. Phonon mode frequencies (in cm⁻¹) of YBaCuFeO₅ (*P4mm*) as obtained from polarized Raman spectra, FIR absorption, Kramers-Kronig analysis (KKA) of FIR reflectance, and lattice dynamical calculations (LDC) using a shell model.

Mode	Raman frequency			Infrared frequency			Lattice dynamics		Main atomic vibrations
	zz	xx	zx,xz	Abs. ω_{TO}	KKA ω_{TO}	ω_{LO}	ω_{TO}	ω_{LO}	
<i>A</i> ₁					97	100	110	153	Ba
<i>A</i> ₁	214						203	210	Cu/Fe
<i>A</i> ₁				238	235	241	214	221	Y
<i>A</i> ₁				360	324	378	343	414	O2-Cu/Fe
<i>A</i> ₁	456						454	454	O2 in phase
<i>A</i> ₁	669	669	669	650	650	664	653	676	O1
<i>B</i> ₁		180						178	O2 out of phase
<i>B</i> ₁		345						340	O2 out of phase
<i>E</i>					122	130	103	114	Ba
<i>E</i>			142		158	171	140	141	Cu/Fe
<i>E</i>			192	192	184	199	187	194	Y
<i>E</i>			280	276	272	280	292	299	O1
<i>E</i>			320				323	340	O2-Cu/Fe
<i>E</i>				360	383	444	361	453	O2-Cu/Fe
<i>E</i>				545			531	541	O2-Cu/Fe
<i>E</i>				576	568	562	571	589	O2-Cu/Fe

function (Fig. 5). The frequencies, so obtained, are also listed in Table III. With a few exceptions there is a good coincidence between the TO frequencies obtained from the absorption maxima and via the Kramers-Kronig procedure.

In the low-frequency range where, following our lattice dynamical calculations (LDC), the *A*₁ and *E* modes related mainly to Ba motions are expected, only reflectance data are available. We connect with these modes the two maxima in Im[$\epsilon(\omega)$] at 97 and 122 cm⁻¹ in close correspondence with the pair of phonons at 107 cm⁻¹ (*A*_{2u}) and 118 cm⁻¹ (*E*_u) observed in tetragonal 123 samples by Crawford *et al.*⁹

We assign the zz-polarized Raman line at 214 cm⁻¹ to the Cu/Fe vibrations of *A*₁ symmetry. In the Raman spectra of YBa₂Cu₃O₆ the like corresponding to the stretching vibrations of Cu (\equiv Cu2) along the *c* axis appears at 140 cm⁻¹ and it is mostly xx-polarized,¹⁰ whereas for the orthorhombic YBa₂Cu₃O₇ it is zz-polarized and shifts to higher wave numbers (149 cm⁻¹). Although the Cu-O2 (Fe-O2) bond lengths remain practically the same, in the case of YBaCuFeO₅ one expects the Cu/Fe (*A*₁) mode to harden, as a result of significant shortening of the Cu-O1 (Fe-O1) bond lengths. The calculated frequency of 203 cm⁻¹ supports our assignment. The larger half-width, compared to that of the Cu2 line in YBa₂Cu₃O₆, may be due to Cu/Fe disorder. The *A*₁ mode of Cu/Fe is observed neither in the absorption nor in the reflectance spectra.

Following the results of LDC, the line at 142 cm⁻¹, obtained in the cross-polarized *xz* and *zx* Raman spectra, corresponds to the *E* mode involving motion of Cu/Fe atoms in the Cu/Fe-O2 planes. For the tetragonal 123 system this mode has been observed by Hadjiev *et al.*¹¹ at 145 cm⁻¹, whereas for the orthorhombic YBa₂Cu₃O₇

the corresponding *B*₂-*B*₃ doublet has been found by McCarty *et al.*¹² at 140 and 142 cm⁻¹. A peak at 145 cm⁻¹ has also been observed in the *y*(*zx*) \bar{y} and *y*(*xz*) \bar{y} Raman spectra of the closely related YBa₂(Cu_{1-x}Fe_x)₃O_{7+ δ} ¹³ and Y_{1-x}Pr_xBa₂Cu₃O_{7- δ} ¹⁴ systems. The Cu/Fe mode of *E* symmetry is pronounced also in the FIR spectra of YBaCuFeO₅ and the Kramers-Kronig analysis yields for its TO frequency the value of 158 cm⁻¹. The discrepancy between the Raman and the KKA frequencies could be explained by the weakness of the corresponding feature in the reflectance spectrum, resulting in a relatively big uncertainty when calculating the frequency of this particular maximum in Im[$\epsilon(\omega)$].

The next *A*₁-*E* pair is the one related to vibrations of Y. The yttrium *A*₁ line is not pronounced in the Raman spectra. We note here that the corresponding mode in the 123 compounds is of *A*_u (*A*_{1u}) symmetry and is Raman-forbidden, although it could be activated, e.g., by hydrogenization (for H_{1.0}YBa₂Cu₃O_{6.7}, Hadjiev *et al.*¹⁵ observed a zz-polarized Raman line of Y vibrations at 210 cm⁻¹). Both *A*₁ and *E* lines are observed in absorption (at 238 cm⁻¹ and 192 cm⁻¹) and reflectance. The LDC frequencies are close to those obtained from the experiment. For the tetragonal 123 phase the Y modes frequencies, as obtained from absorption⁸ and reflectance⁹ spectra, are at 218 (*A*_{2u}) and 192 cm⁻¹ (*E*_u).

The assignment of the Raman lines at 345 cm⁻¹ (xx-polarized) and at 456 cm⁻¹ (zz-polarized) to the even out-of-phase and in-phase vibrations of O2 atoms along the *c* axis, respectively, is most straightforward. Indeed, the corresponding modes in YBa₂Cu₃O_{6+ δ} are observed at 340 and 450 cm⁻¹ and have the same polarizations.¹⁰ Moreover, the observation of the 345 cm⁻¹ line in the *c*(*a*+*b*,*a*-*b*) \bar{c} spectrum and its absence in

$c(a+b, a+b)\bar{c}$ clearly indicates B_1 symmetry ($\alpha_{xx} = -\alpha_{yy}, \alpha_{zz} \approx 0$). The band at 180 cm^{-1} (xx -polarized) shows the same B_1 -type behavior and we assign it to the odd out-of-phase B_1 mode, strictly Raman active in the case of the $P4mm$ space group, which is another evidence for this space group. This mode corresponds to the odd B_{1u} mode in the tetragonal 123 compounds, where it is silent, because the net dipole vector is zero. If one accepts the $P4/mmm$ space group, this mode is of B_{2u} -type with a small net dipole moment. In the case of the $P4mm$ space group the displacements are not equal and this mode can be activated and observed in the xx -polarized Raman spectrum. It follows from our calculations of the lattice dynamics that the frequency of this mode is 180 cm^{-1} . Earlier calculations¹⁶ of the frequency of the B_{1u} mode in the orthorhombic 123 phase have yielded the value of 313 cm^{-1} , but no IR phonon line has been found near this frequency. There is another phonon mode of A_1 symmetry involving motions of O2 and Cu/Fe atoms along the c direction, which has not been observed in the xx - or zz -Raman spectra. This mode is Raman-forbidden (B_{2u}) for the centrosymmetric $Pmmm$ or $P4/mmm$ structures of the 123 compounds, and, following the calculations of the lattice dynamics (see Table III), its frequency (343 cm^{-1}) is very close to two other modes of E symmetry (323 and 361 cm^{-1}). In the nonpolarized IR absorption and reflectance spectra, the phonon bands related to these three modes should be superimposed, and hence their separation is not possible at present.

Following the LDC analysis, one expects four modes of E symmetry that involve vibrations of large amplitude of O2 atoms in the ab plane. The two strong absorption bands at 360 and 568 cm^{-1} (there is a weak Raman line at 576 cm^{-1} in the xz and zx spectra) could be assigned to the odd in-phase and out-of-phase in-plane Cu/Fe-O2 vibrations, respectively. The bands are relatively broad and, as discussed above, the one at 360 cm^{-1} could be a superposition of one A_1 and two E bands. The corresponding IR absorption band for the $\text{YBa}_2\text{Cu}_3\text{O}_6$ system is also broad and at nearly the same frequency (368 cm^{-1}).

While the E modes at 360 and 568 cm^{-1} correspond to the odd E_u (B_{2u} - B_{3u}) modes of the 123 systems, there are two other (even) modes involving O2 motions that are of E_g (B_{2g} - B_{3g}) symmetry in the 123 system but are of E symmetry for the $P4mm$ structure of YBaCuFeO_5 . The LDC¹⁶ predict for their frequencies 323 and 531 cm^{-1} and we do observe weak xz - and zx -polarized Raman features at 320 and 545 cm^{-1} . It seems that in the IR spectra, these bands are obscured by the much stronger E bands originating from the E_u (B_{2u} - B_{3u}) modes.

The only modes of the $P4mm$ structure still unidentified are the A_1 and E modes involving mainly vibrations of the apex oxygen (O1) along the c axis and in the Ba-O1 plane, respectively. Consistent with our LDC results, we accept that the A_1 mode of O1 is represented by the strong mostly zz -polarized Raman line 669 cm^{-1} and by the lines in the IR absorption spectra with $\omega_{\text{TO}} \approx 650 \text{ cm}^{-1}$. Within the $P4/mmm$ space group, this

mode would be Raman-forbidden, and hence its appearance is another evidence that the structure of YBaCuFeO_5 is described by the $P4mm$ space group. The TO frequency of this mode corresponds to the one in 123 measured⁹ at 648 cm^{-1} . It is well known that the frequency of the Raman active mode of the O1 atom vibrations in the 123 system is very sensitive to the apex oxygen content. With increasing the laser power (temperature), both the peak area and frequency decrease, similarly for the case of the Raman line at 500 cm^{-1} in the $\text{YBa}_2(\text{Cu}_{1-x}\text{Fe}_x)_3\text{O}_{7+\delta}$ system.¹³ From the comparison of the $y(zz)\bar{y}$ and $y(xx)\bar{y}$ scattering cross sections, one concludes that for this mode, $S_{zz} \approx 7S_{xx} \approx 7S_{yy}$.

The peak at 669 cm^{-1} is more intensive in $y(zx)\bar{y}$ than in $y(xz)\bar{y}$ polarization geometries and that shows possible "polarization leakage" in these configurations of the Raman spectra.

The weak xz - and zx -polarized Raman feature near 280 cm^{-1} and the absorption maximum at 276 cm^{-1} could be assigned to the E mode of the O1 vibrations in Ba-O1 planes. Lattice dynamics⁷ of the tetragonal 123 system has given for this mode a frequency of 365 cm^{-1} which is higher than the real value. Indeed, for the orthorhombic 123 system the B_{2g} - B_{3g} pair has been observed¹² at 210 and 303 cm^{-1} , respectively. In the tetragonal phase the splitting has to decrease and the lines should merge into a single E_g model which was observed recently by Hadjiev *et al.*¹¹ at 310 cm^{-1} . The lattice dynamical calculations for YBaCuFeO_5 give a frequency of 272 cm^{-1} , which is in excellent agreement with the experimentally observed frequencies.

At last we shall discuss the possible origin of the strong Raman line at 576 cm^{-1} which cannot be included in the above-described classification of the Γ -point phonons of YBaCuFeO_5 because all normal modes have already been assigned and the lattice dynamic calculations give no indication for an A_1 mode of close frequency.

Unpolarized or zz -polarized Raman line at about 576 cm^{-1} has been observed in the spectra of a number of layered oxide compounds such as $\text{YBa}_2\text{Cu}_3\text{O}_{6+\delta}$,^{12,17-19} $\text{YBa}_2(\text{Cu}_{1-x}\text{Co}_x)\text{O}_{7-\delta}$,²⁰ $\text{YBa}_2(\text{Cu}_{1-x}\text{Fe}_x)\text{O}_{7-\delta}$,¹³ $\text{Y}_{1-x}\text{Pr}_x\text{Ba}_2\text{Cu}_3\text{O}_{7-\delta}$,¹⁴ $\text{La}_{2-x}\text{Sr}_x\text{CaCu}_2\text{O}_6$,²¹ and $\text{Nd}_{2-x}\text{Ce}_x\text{CuO}_4$.²² It has been noted that the relative intensity of this line increases with cation substitution and/or with oxygen nonstoichiometry and does not change in frequency at the phase transition. In most cases its appearance in the 123 compounds has been attributed to disorder-activated infrared mode along the c axis, associated with the apex oxygen O1 or the oxygen atoms O4 in the chains. Such arguments are obviously not valid in our case as all normal modes are both Raman and IR allowed and, despite the closeness to the frequency of one of the E modes, the Raman line at 576 cm^{-1} is much stronger in a parallel scattering configuration (an E mode should be stronger in the crossed zx and xz spectra). Heyen *et al.*²³ have observed in $\text{NdBa}_2\text{Cu}_3\text{O}_{7-\delta}$ a peak at 555 cm^{-1} that has not followed any polarization selection rules and assumed that it is of phonon density-of-states origin. The same assumption has been made by Thomsen *et al.*²⁴ for the line at 550 cm^{-1} in the

PrBa₂Cu₃O_{7-δ} system and by Iliev *et al.*^{13,14} for the line at 580 cm⁻¹ in YBa₂(Cu_{1-x}Fe_x)O_{7+δ} and Y_{1-x}Pr_xBa₂Cu₃O_{7-δ} systems.

We measured the Raman spectra of YBaCuFeO₅ at various laser powers, i.e., at different temperatures, and found that although the line at 576 cm⁻¹ broadened significantly with increasing temperature, its frequency remained practically unchanged. Using the same arguments as in Ref. 13, it is reasonable to assume that the unpolarized 576 cm⁻¹ line in the Raman spectra of YBaCuFeO₅ is due to partial disorder and corresponds to a maximum of the phonon density of states. If this is so, the high frequency suggests that the line could be related to the phonon branches of oxygen (O1 and/or O2). It is worth noting that in some studies on 123 compounds, the disorder-induced line at 570–590 cm⁻¹ has been attributed to the “chain” oxygen, which is absent in the YBaCuFeO₅ structure.

CONCLUSION

In conclusion, from the polarized Raman scattering, FIR absorption and reflectance of all Γ -point phonons expected for the insulating ferromagnetic with *P4mm* structure YBaCuFeO₅ have been identified. The phonon frequencies are compared to those obtained from calculations of the lattice dynamics using a shell model. The experimental and theoretical results are discussed in close comparison with the available data for YBa₂Cu₃O_{7-δ}, taking into account the similarity of both structures.

ACKNOWLEDGMENTS

We thank M. Gyulmezov for the FIR measurements, M. Tumangelova for the TEM analysis and L. Georgieva for her expert technical help. This work was supported in part by Grants No. F1/91 and No. F2/91 (2001 and 2002) of the Bulgarian National Foundation for Science.

-
- ¹L. Er-Rakho, C. Michel, P. Lacorre, and B. Raveau, *J. Solid State Chem.* **73**, 531 (1988).
- ²C. Meyer, F. Hartmann-Boutron, Y. Gros, and R. Strobel, *Solid State Commun.* **76**, 163 (1990).
- ³C. Mitros, V. Psycharis, M. Pissas, and D. Niarchos, in *Proceedings of the First General Conference of the Balkan Physical Union*, 1991, edited by K. M. Paraskevopoulos (Hellenic Physical Society, Thessaloniki, 1992), Vol. II, p. 993.
- ⁴M. Pissas, C. Mitros, G. Kallias, V. Psycharis, D. Niarchos, A. Simopoulos, A. Kostikas, C. Christides, and K. Prassides, *Physica C* **185-189**, 185 (1991).
- ⁵V. N. Popov and V. L. Valchinov, *Physica C* **172**, 260 (1990); G. A. Zlateva, V. N. Popov, M. Gyulmezov, L. N. Bozukov, and M. N. Iliev, *J. Phys. Condens. Matter* **4**, 8543 (1992); V. N. Popov (unpublished).
- ⁶P. Bordet, C. Chaillout, J. J. Capponi, J. Chenavas, and M. Marezio, *Nature* **327**, 687 (1987).
- ⁷F. Bates, *Phys. Rev. B* **39**, 322 (1989).
- ⁸G. Burns, F. H. Dacol, P. Freitas, T. S. Plaskett, and W. Knig, *Solid State Commun.* **64**, 471 (1987).
- ⁹M. K. Crawford, G. Burns, and F. Holtzberg, *Solid State Commun.* **70**, 557 (1989).
- ¹⁰V. G. Hadjiev, M. N. Iliev, and P. G. Vassilev, *Physica C* **153-155**, 290 (1988).
- ¹¹V. J. Hadjiev, C. Thomsen, and M. Cardona, in *Proceedings of the XIIIth International Conference on Raman Spectroscopy*, 1992, edited by W. Kiefer, M. Cardona, G. Schaack, F. W. Schneider, and H. W. Schrötter (Wiley, Chichester, 1992), p. 878.
- ¹²K. F. McCarty, J. Z. Liu, R. N. Shelton, and H. B. Radousky, *Phys. Rev. B* **41**, 8792 (1990).
- ¹³M. N. Iliev, Y. K. Atanassova, L. Bozukov, J. Tihov, V. G. Hadjiev, and E. Liarokapis, *Physica C* **191**, 419 (1992).
- ¹⁴M. N. Iliev, G. A. Zlateva, P. Nozar, and P. Stastny, *Physica C* **191**, 477 (1992).
- ¹⁵V. G. Hadjiev, M. V. Abrashev, M. N. Iliev, and L. N. Bozukov, *Physica C* **171**, 257 (1990).
- ¹⁶W. Kress, U. Schröder, J. Prade, A. D. Kulkani, and F. W. de Wette, *Phys. Rev. B* **38**, 2906 (1988).
- ¹⁷V. N. Denisov, B. N. Mavrin, V. B. Podoberov, I. V. Alexandrov, A. B. Bykov, A. F. Goncharov, and O. K. Mel'nikov, *Phys. Lett. A* **130**, 411 (1988).
- ¹⁸K. F. McCarty, J. C. Hamilton, R. N. Shelton, and D. S. Ginley, *Phys. Rev. B* **38**, 2914 (1988).
- ¹⁹G. Burns, F. H. Dacol, C. Feild, and F. Holtzberg, *Solid State Commun.* **75**, 893 (1990).
- ²⁰A. Erle and G. Güntherodt, *Physica C* **171**, 216 (1990).
- ²¹D. M. Mateev, M. N. Iliev, L. N. Bozukov, V. G. Hadjiev, and P. Stastny, *Physica C* **179**, 295 (1991).
- ²²V. G. Hadjiev, I. Z. Kostadinov, L. Bozukov, E. Dinolova, and D. M. Mateev, *Solid State Commun.* **71**, 1093 (1989).
- ²³E. T. Heyen, R. Wegerer, E. Schonherr, and M. Cardona, *Phys. Rev. B* **44**, 10195 (1991).
- ²⁴C. Thomsen, R. Liu, and M. Cardona, *Solid State Commun.* **67**, 271 (1988).